ORIGINAL ARTICLE

# Synthesis and Physicochemical Characterization of Naringenin- and Gallic Acid-Loaded Polymeric Micelles for Cancer Drug Delivery

Khaliqah Syafiqah Basir[1], Husnul Mufida[1], Norjihada Izzah Ismail[1,2]

[1] School of Biomedical Engineering and Health Sciences, Faculty of Engineering, Universiti Teknologi Malaysia, 81310 UTM Johor Bahru, Johor, Malaysia.
[2] Medical Devices and Technology Centre, Institute of Human Centered Engineering, Universiti Teknologi Malaysia, 81310 UTM Johor Bahru, Johor, Malaysia.

## ABSTRACT

**Introduction:** Cancer nano-drug drug delivery system is important as it can improve drug bioavailability and reduce dosing frequency. Polymeric micelles (PMs) can reach targeted site and most likely will be useful in reducing side effects of treatment. This study aimed to synthesize naringenin- and gallic acid-loaded polymeric micelles for cancer drug delivery and to determine their physicochemical properties including particle size, polydispersity index (PDI) and structural composition. **Methods:** Two types of PMs (naringenin [NAR] and gallic acid [GA]) were prepared in different proportions of polyethylene glycol (PEG) and D-α-tocopheryl polyethylene glycol 1000 succinate (TPGS) via solvent casting method. These PMs were visually observed and further analyzed by dynamic light scaterring (DLS) and fourier-transform infrared spectroscopy (FTIR) techniques. **Results:** From this study, NAR-PEG-TPGS PMs showed particle size less than 30 nm whereas GA-PEG-TPGS PMs exhibited larger particle size between 171-205 nm. NAR2 PM that contain higher amount of TPGS were observed to have smaller particle size whereas GA2 PM with higher TPGS content exhibited larger particle size. PDI values for these drug-loaded PMs were between 0.32-0.74. FTIR results confirmed the presence of O-H and C=O stretching vibrations in all PM samples. **Conclusion:** NAR-PEG-TPGS PMs had shown more relevant physicochemical properties than GA-PEG-TPGS PMs for cancer nano-drug delivery.

**Keywords:** Drug delivery, Polymeric micelles, Naringenin, Gallic acid, Cancer

**Corresponding Author:**
Norjihada Izzah Ismail, PhD
Email: norjihada@utm.my

## INTRODUCTION

Listed as the second common causes of mortality, cancer has resulted in a large number of deaths each year (1). Cancer can be caused by changes in the genes that control the way cell functioning. These result in uncontrolled cell growths forming tumor that can metastasize to different areas of the body and may require chemotherapy as one of the treatment options. Due to the undesirable side effects of conventional chemotherapy, nano-drug delivery systems are extensively studied in order to enhance drug efficacy and/or reduce drug toxicity (2,3). In fact, nanoparticles has getting much attention these days for use in drug delivery as drug nanocarriers, mainly due to their smaller particle size which is commonly less than 100 nm but can as well be up to several hundred nanometers in size (3,4). Various types of nanoparticles are available including polymeric micelles, liposomes, niosomes, magnetic nanoparticles, solid lipid nanoparticles, dendrimers, carbon nanoparticles, nanosheets and so forth (3-5). Utilization of nanoparticles in cancer drug delivery gives advantages such as lower treatment dose, specific targeting of drug towards tumor site and minimize adverse side effects to the patients (2,3,6). Interestingly, smaller nanoparticles (< 150 nm) may be able to escape clearance by the reticuloendothelial system (RES) than larger-sized particles (7,8). However, it is suggested that the nanoparticles must be large enough (up to 100 nm) to prevent rapid leakage of drug nanoparticles into blood capillaries (7). Also, particles smaller than 10 nm are subjected to renal filtration and are not reabsorbed (8), thus highlighting the importance of optimal size of drug carriers for nano-drug delivery.

Polymeric micelles (PMs) are nanostructures which consist of a hydrophobic core and a hydrophilic shell. This core-shell structure is formed via self-assembly of co-polymer used (9). The hydrophobic core of PMs is able to entrap the poorly water soluble drugs whereas its hydrophilic shell provides protection from external

environment (9). Drug encapsulation within micelles core can be achieved through electrostatic, physical or chemical interactions (5). Different types of co-polymer such as poly(ethylene glycol) (PEG), poly(ε-caprolactone) (PCL), and D-α-tocopheryl polyethylene glycol 1000 succinate (TPGS) have been studied in the formulation of cancer drug-loaded PMs (10,11). It is noteworthy that PMs are able to enhance drug bioavalability and biodistribution (9).

Naringenin (NAR) is a flavonoid under the class flavanone and can be found mostly in citrus fruits (12). Gallic acid (GA) on the other hand, is a phenolic acid. Both NAR and GA are polyphenols that have been known to exert various biological properties such as antioxidant, anti-inflammatory, anticancer and cardioprotective (12-17). The anticancer activity of NAR and GA was attributed to their capacity to induce cytotoxicity and apoptosis (15,17). Very limited number of study on NAR PMs has been conducted (18), but nano-drug delivery of NAR has often been studied in the form of nanoparticles (NPs) such as NAR-loaded chitosan NPs (19) and NAR-loaded gelatin-coated PCL NPs (20). GA has been co-delivered with cancer chemotherapy drug Doxorubicin using polyethylene glycol-distearoyl phosphoethanolamine (PEG-DSPE), lecithin and PCL to form lipid-polymer hybrid nanoparticles (21) while gum Arabic has been used to synthesize GA NPs (22). However, the physicochemical properties of NAR or GA in combination with TPGS and PEG in the form of polymeric micelles are still unknown. The presence of TPGS is expected to enhance nanocarrier stability and act as P-glycoprotein inhibitors whereas the PEG helps prolong drug circulation in the plasma (11,23). Thus, this study was conducted to synthesize the NAR and GA PMs using TPGS and PEG and characterize some of their physicochemical properties for potential use as new cancer nano-drug delivery systems.

## MATERIALS AND METHODS

### Materials

Naringenin (MW = 272.3, purity ≥98%), gallic acid (MW = 188.13, purity ≥98%), PEG, TPGS, phosphate-buffered saline (PBS) and chloroform were purchased from Sigma-Aldrich.

### Synthesis of polymeric micelles

NAR-PEG-TPGS PMs and GA-PEG-TPGS PMs were prepared according to Muthu et al. (10) with modifications. All PM samples were synthesized following the formulations provided in Table I. Variations were made in order to identify the compositions that provide ideal physicochemical properties for used as cancer nano-drug delivery systems. NAR or GA, PEG and TPGS were dissolved in 3 mL of chloroform. The chloroform was then evaporated by immersing the mixture in a 40 °C water bath. Fifteen mL of 0.1 M PBS pH 7.4 was added to the resulting thin layer of drug-dispersed PEG-TPGS and this mixture was incubated at 37 °C for 48 hours. The final solution of PMs was then filtered using 0.2 µm syringe filter to remove non-incorporated drug. All PM samples were stored at 4 °C until further use.

**Table I: Formulations of polymeric micelles.**

| PM samples | Ratio PEG:T-PGS | NAR/GA (mg) | PEG (mg) | TPGS (mg) |
|---|---|---|---|---|
| Blank PEG-TPGS (B1) | 1:1 | - | 50 | 50 |
| Blank PEG-TPGS (B2) | 1:2 | - | 50 | 100 |
| NAR-PEG-TPGS (NAR1) | 1:1 | 2.5 | 50 | 50 |
| NAR-PEG-TPGS (NAR2) | 1:2 | 2.5 | 50 | 100 |
| GA-PEG-TPGS (GA1) | 1:1 | 2.5 | 50 | 50 |
| GA-PEG-TPGS (GA2) | 1:2 | 2.5 | 50 | 100 |

B = blank, GA = gallic acid; NAR = naringenin; PEG = poly(ethylene glycol); TPGS = D-ε-to-copheryl polyethylene glycol succinate.

### Visual observation of polymeric micelles

All PMs were observed visually using naked eye for any colour changes after 24 hours of synthesis and upon storage for 10 days at 4 °C.

### Physicochemical analyses of polymeric micelles

Particle size and PDI of all PMs were measured using a Zetasizer Nano ZSP (Malvern Instruments, UK). All samples were analyzed in triplicates and mean values were calculated. The functional groups and bonds of each PMs were determined using a FTIR spectrometer in the region of 400 to 4000 $cm^{-1}$.

## RESULTS

### Visual observation of polymeric micelles

From the visual observation using unaided eye, blank B1 and B2 PMs as well as NAR-loaded PMs NAR1 and NAR2 were light brown in colour and transparent after 24 hours of synthesis. These PMs' colours remained the same after 10 days of storage. However, colour changes were observed for GA-loaded PMs GA1 and GA2 from colorless after 24 hours of synthesis to dark green colour upon storage for 10 days. Fig. 1 depicts the colour appearance of several PM samples.

### Particle size and polydispersity index

Particle size and polydispersity index (PDI) of all PM samples were shown in Table II. GA-PEG-TPGS PMs showed larger particle size (> 100 nm) than the NAR-PEG-TPGS PMs. The lowest PDI was seen in B1 sample whereas the highest was shown by NAR1 sample.

### Structural composition of polymeric micelles

FTIR results of NAR-PEG-TPGS PMs and GA-PEG-TPGS PMs were presented in Fig. 2 and Fig. 3, respectively. No clear peak differences were seen between blank

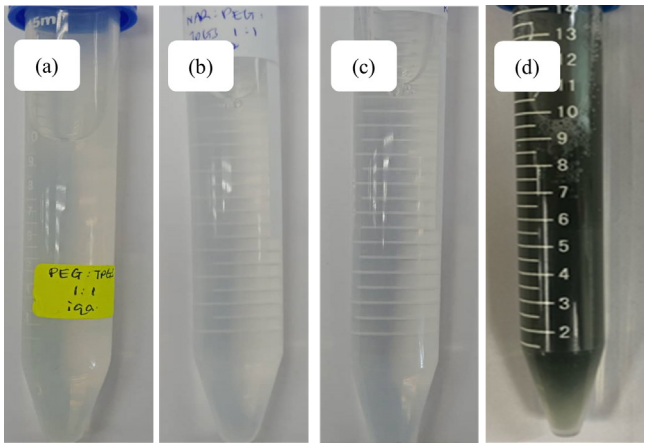


**Figure 1: Colour appearance of PM samples: (a) B1, (b) NAR1, (c) NAR2 and (d) GA1 after storage for 10 days**

**Table II: Particle size and polydispersity index of polymeric micelles**

| PM samples | Ratio PEG:TPGS | Particle size (d.nm) (mean ± SD) | PDI (mean ± SD) |
|---|---|---|---|
| B1 | 1:1 | 15.86 ± 0.45 | 0.29 ± 0.02 |
| B2 | 1:2 | 27.76 ± 0.09 | 0.69 ± 0.00 |
| NAR1 | 1:1 | 28.84 ± 0.16 | 0.74 ± 0.01 |
| NAR2 | 1:2 | 17.70 ± 0.20 | 0.32 ± 0.00 |
| GA1 | 1:1 | 171.23 ± 1.84 | 0.66 ± 0.00 |
| GA2 | 1:2 | 204.80 ± 2.48 | 0.48 ± 0.04 |

B = blank, NAR = Naringenin; GA = Gallic acid; PDI = polydispersity index, PEG = Poly(ethylene glycol); TPGS = D-ε-Tocopheryl polyethylene glycol succinate, SD = standard deviation.

PMs and NAR-PEG-TPGS PMs (Fig. 2). The FTIR spectra displayed a strong absorption band at 3321 $cm^{-1}$ and 1634 $cm^{-1}$, referring to O-H and C=O stretching, respectively. In comparison, both GA1 and GA2 samples showed a peak at 1016 $cm^{-1}$ which was absent in blank B1 and B2 samples (Fig. 3). This peak refers to C-O stretching vibration of gallic acid.

## DISCUSSION

The results of visual observation suggested that oxidation of GA could have taken place following storage of GA-PEG-TPGS PMs. Earlier study reported similar observations where their GA solutions at pH 7.2 changed colour from almost colourless with a slight yellow tint (t=0) to green and brown after 1 and 30 days of storage at 23 °C, respectively (24). The oxidation of GA as observed from the colour changes could indicate that GA has been degraded to form its oxidation products (25).

The particle sizes of NAR-PEG-TPGS PMs seen in this study were smaller than reported studies of NAR-loaded in zeolite imidazole framework (ZIF) PMs which showed average particle size of 203.5 ± 0.85 nm (18). On the other hand, particle sizes of GA-PEG-TPGS PMs observed in this study were within the range of 33 to 250 nm reported for GA-loaded in arabic gum NPs (22). For cancer drug delivery systems, smaller nanoparticles

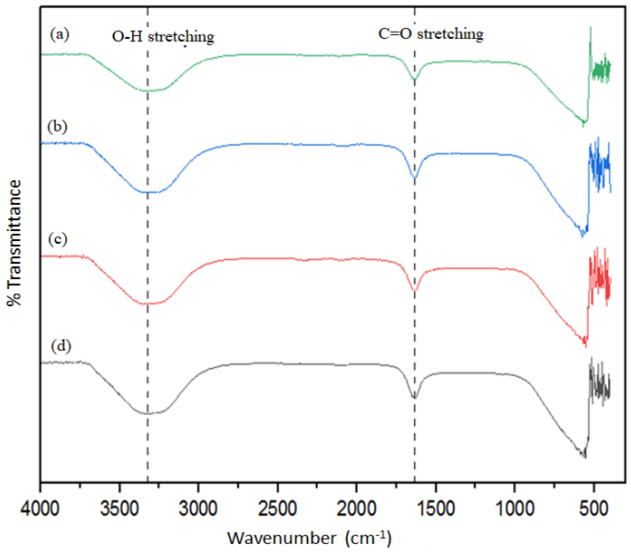


**Figure 2: FTIR spectra of NAR-PEG-TPGS PM and blank samples: (a) NAR2, (b) NAR1, (c) B2 and (d) B1**

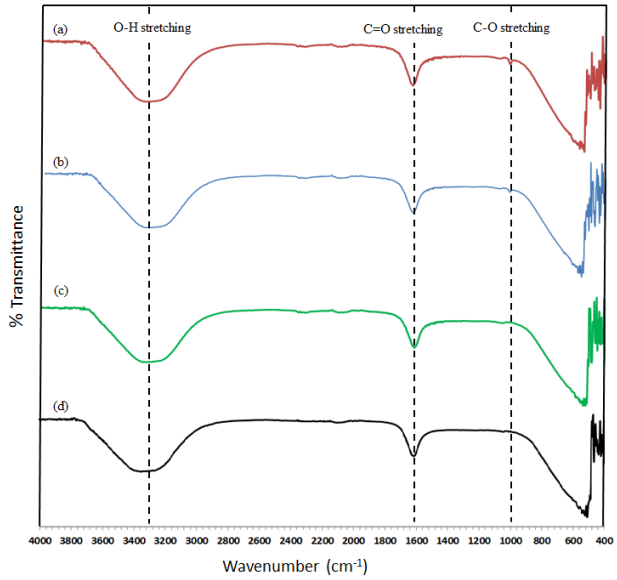


**Figure 3: FTIR spectra of GA-PEG-TPGS PM and blank samples: (a) GA2, (b) GA1, (c) B2 and (d) B1.**

between 10-100 nm are desirable to avoid renal filtration and clearance by fixed macrophages found in the RES (8). Surprisingly, complement activation can also be triggered by nanoparticles with diameter greater than 200 nm, resulting in rapid removal of these large-sized molecules from the bloodstream via different uptake routes such as caveolin- or clathrin-mediated endocytosis (26,27). Particles with size between 250 nm to 3μm are subjected to uptake via phagocytosis (26). However, the presence of PEG in the hydrophilic shell gives advantages to the polymeric micelle. Specifically, hydrophilicity and flexibility of PEG reduce nonspecific interactions with protein and opsonisation which may promote micelle clearance by RES (28).

It can be observed from Table 2 that increasing ratio of

PEG:TPGS from 1:1 to 1:2 increased the particle size of blank PMs and GA-PEG-TPGS PMs. These findings were in agreement with an earlier study by Md et al. (19). Addition of more TPGS resulted in higher portion of hydrophilic moiety of the polymeric micelles than the hydrophobic moiety and drug. The greater particle size seen for GA2 as compared to GA1 could be due to the higher PEG-TPGS chains per volume. Consequently, interactions between GA and PEG-TPGS were affected where stronger intermolecular hydrogen bonding attraction, decreased intermolecular distance and insufficient electrostatic repulsion resulted in larger particle size of PMs (19).

However, dissimilar observation was seen for NAR2 PM which showed smaller particles than blank B2 sample. Size of micelles in aqueous solution was influenced by several factors including polymer weight and amount of drug loaded into the micelles (28). In fact, drug-polymer interactions in the micelles occur via hydrophobic interactions, hydrogen bonding and pi-pi interactions (28). PDI values for all samples exceed 0.3 except for blank B1 PM (Table 2). In the presence of more TPGS as seen in NAR2 and GA2 PMs, slightly lower PDI values were obtained. Micelles with PDI values closer to 1 as shown by B2, NAR1 and GA1 PMs indicated that these samples had polydisperse distributions (8) whereas B1, NAR2 and GA2 PMs were moderately polydispersed. On the contrary, the micelles with smaller PDI values of 0.2 and below are suitable for polymer-based nanoparticle materials due to their monodisperse distribution (8).

It can be seen that sharp peaks of hydroxyl group and carbonyl group were found at 3304-3321 $cm^{-1}$ and 1634-1635 $cm^{-1}$, respectively (Fig. 2,3). A previous study reported that naringenin exhibited absorption peaks of O-H stretching vibration at 3285 $cm^{-1}$ and C=O stretching vibration at 1629 $cm^{-1}$ (29). PEG and TPGS were shown to exhibit hydroxyl groups at 3417 $cm^{-1}$ and 3452-3454 $cm^{-1}$, respectively (11,30). The characteristics band for the C=O stretching vibration of carbonyl group appeared at 1630 $cm^{-1}$ for PEG (30) and at 1737-1738 $cm^{-1}$ for TPGS (11). Similarly, O-H band was seen at 3409 $cm^{-1}$ for the gallic acid while C=O stretching vibration was observed at 1681 $cm^{-1}$ (13). Additionally, the peak at 1016 $cm^{-1}$ observed in GA1 and GA2 samples refers to C-O stretching vibration of gallic acid where in an earlier study it was seen at 1026-1028 $cm^{-1}$ (13,31). Therefore, the FTIR results confirm the presence of OH and C=O groups in all PM samples were contributed by NAR, GA, PEG and TPGS.

## CONCLUSION

It can be concluded from this study that NAR1 and NAR2 PMs exhibited desired physicochemical properties as new drug delivery systems attributed by their smaller particle sizes than GA1 and GA2 PMs. However, due to the larger PDI value of NAR1 PM, NAR2 PM is considered having optimal physicochemical properties as new drug delivery system. Smaller-sized polymeric micelles give better biodistribution as these particles can reach tumor target site through leaky vasculature as well as can avoid clearance in the systemic circulation.

## ACKNOWLEDGEMENTS

This work was financially supported by the Universiti Teknologi Malaysia under the Research University Grant and the Ministry of Higher Education Malaysia with reference number R.J130000.2651.17J40. Authors thank School of Biomedical Engineering and Health Sciences, Universiti Teknologi Malaysia for the provided equipment.

## REFERENCES

1. Islami F, Goding Sauer A, Miller KD, Siegel RL, Fedewa SA, Jacobs EJ, McCullough ML, Patel AV, Ma J, Soerjomataram I, Flanders WD, Brawley OW, Gapstur SM, Jemal A. Proportion and number of cancer cases and deaths attributable to potentially modifiable risk factors in the United States. A Cancer Journal for Clinicians. 2018;68(1):31-54.
2. Liu L, Ye Q, Lu M, Chen S-T, Tseng H-W, Lo Y-C, Ho C. A new approach to deliver anti-cancer nanodrugs with reduced off-target toxicities and improved efficiency by temporarily blunting the reticuloendothelial system with intralipid. Scientific Reports, 2017;7(1):16106.
3. Senapati S, Mahanta AK, Kumar S, Maiti P. Controlled drug delivery vehicles for cancer treatment and their performance. Signal Transduction and Targeted Therapy. 2018;3(1):7.
4. Chenthamara D, Subramaniam S, Ramakrishnan SG, Krishnaswamy S, Essa MM, Lin F.-H, Qoronfleh MW. Therapeutic efficacy of nanoparticles and routes of administration. Biomaterials Research. 2019;23(1):20.
5. Singh AP, Biswas A, Shukla A, Maiti P. Targeted therapy in chronic diseases using nanomaterial-based drug delivery vehicles. Signal Transduction and Targeted Therapy. 2019;4(1):33.
6. Yan L, Shen J, Wang J, Yang X, Dong S, Lu S. Nanoparticle-based drug delivery system: A patient-friendly chemotherapy for oncology. Dose-Response. 2020:1-12.
7. Dadwal A, Baldi A, Narang RK. Nanoparticles as carriers for drug delivery in cancer. Artificial Cells, Nanomedicine, and Biotechnology. 2018;46:295-305.
8. Danaei M, Dehghankhold M, Ataei S, Davarani FH, Javanmard R, Dokhani A, Khorasani S, Mozafari MR. Impact of particle size and polydispersity index on the clinical applications of lipidic nanocarrier systems. Pharmaceutics. 2018;10(2):57.
9. Yu G, Ning Q, Mo Z, Tang S. Intelligent polymeric micelles for multidrug co-delivery and cancer

therapy. Artificial Cells, Nanomedicine, and Biotechnology. 2019;47(1):1476-1487.
10. Muthu MS, Kulkarni, SA, Liu Y, Feng SS. Development of docetaxel-loaded vitamin E TPGS micelles: Formulation optimization, effects on brain cancer cells and biodistribution in rats. Nanomedicine. 2012;7(3):353-364.
11. Yusuf O, Ali R, Alomrani AH, Alshamsan A, Alshememry AK, Almalik AM, Lavasanifar A, Binkhathlan Z. Design and development of D-α-tocopheryl polyethylene glycol succinate-block-poly(ε-caprolactone) (TPGS–b–PCL) nanocarriers for solubilization and controlled release of Paclitaxel. Molecules. 2021;26:2690.
12. Testai L, Da Pozzo E, Piano I, Pistelli L, Gargini C, Breschi MC, Braca A, Martini C, Martelli A, Calderone, V. The citrus flavanone naringenin produces cardioprotective effects in hearts from 1 year old rat, through activation of mitoBK channels. Frontiers in Pharmacology. 2017;8:71.
13. Ismail, NI, Sornambikai S, Kadir MRA, Mahmood NH, Zulkifli RM, Shahir S. Evaluation of radical scavenging capacity of polyphenols found in natural Malaysian honeys by voltammetric techniques. Electroanalysis. 2018;30(12):2939-2949.
14. Hernбndez-Aquino E, Muriel P. Beneficial effects of naringenin in liver diseases: Molecular mechanisms. World Journal of Gastroenterology. 2018;24(16):1679-1707.
15. Aborehab NM, Osama N. Effect of gallic acid in potentiating chemotherapeutic effect of Paclitaxel in HeLa cervical cancer cells. Cancer Cell International. 2019;19:154.
16. Nguyen-Ngo C, Salomon C, Lai A, Willcox JC, Lappas M. Anti-inflammatory effects of gallic acid in human gestational tissues in vitro. Reproduction. 2020;160(4): 561-578.
17. Martнnez-Rodrнguez OP, Gonzбlez-Torres A, Бlvarez-Salas LM, Hernбndez-Sбnchez H, Garcнa-Pйrez BE, Thompson-Bonilla, M del R, Jaramillo-Flores ME. Effect of naringenin and its combination with cisplatin in cell death, proliferation and invasion of cervical cancer spheroids. RSC Advances. 2021;11(1):129-141.
18. Wang Z, Ye X, Fang Y, Cheng H, Xu Y, Wang X. Development and in vitro evaluation of pH-sensitive naringenin@ZIF-8 polymeric micelles mediated by aptamer. Journal of Drug Delivery Science and Technology. 2021;65:102702.
19. Md S, Alhakamy NA, Aldawsari HM, Asfour HZ. Neuroprotective and antioxidant effect of naringenin-loaded nanoparticles for nose-to-brain delivery. Brain Sciences. 2019;9(10):275.
20. Ahmad A, Fauzia E, Kumar M, Mishra RK, Kumar A, Khan MA, Raza SS, Khan, R. Gelatin-coated polycaprolactone nanoparticle-mediated naringenin delivery rescue human mesenchymal stem cells from oxygen glucose deprivation-induced inflammatory stress. ACS Biomaterials Science & Engineering. 2019;5(2):683-695.
21. Shao Y, Luo W, Guo Q, Li X, Zhang Q, Li J. In vitro and in vivo effect of hyaluronic acid modified, doxorubicin and gallic acid co-delivered lipid-polymeric hybrid nano-system for leukemia therapy. Drug Design, Development and Therapy. 2019;13:2043-2055.
22. Hassani A, Azarian MMS, Ibrahim WN, Hussain SA. Preparation, characterization and therapeutic properties of gum arabic-stabilized gallic acid nanoparticles. Scientific Reports. 2020;10(1):17808.
23. Sun C, Li W, Ma P, Li Y, Zhu Y, Zhang H, Adu-Frimpong M, Deng W, Yu J, Xu, X. Development of TPGS/F127/F68 mixed polymeric micelles: Enhanced oral bioavailability and hepatoprotection of syringic acid against carbon tetrachloride-induced hepatotoxicity. Food and Chemical Toxicology. 2020;137:111126.
24. Pant AF, Цzkasikci D, Fьrtauer S, Reinelt M. The effect of deprotonation on the reaction kinetics of an oxygen scavenger based on gallic acid. Frontiers in Chemistry. 2019;7:1-7.
25. Gomes A, Costa ALR, de Assis Perrechil F, da Cunha RL. Role of the phases composition on the incorporation of gallic acid in O/W and W/O emulsions. Journal of Food Engineering. 2016;168:205-214.
26. Biswas AK, Islam MR, Choudhury ZS, Mostafa A, Kadir MF. (2014). Nanotechnology based approaches in cancer therapeutics. Advances in Natural Sciences: Nanoscience and Nanotechnology. 2014;5(4):043001.
27. Hoshyar N, Gray S, Han H, Bao G. The effect of nanoparticle size on in vivo pharmacokinetics and cellular interaction. Nanomedicine. 2016; 11(6):673-692.
28. Hwang D, Ramsey JD, Kabanov AV. Polymeric micelles for the delivery of poorly soluble drugs: From nanoformulation to clinical approval. Advanced Drug Delivery Reviews. 2020;156(1);80-118.
29. Mundlia J, Ahuja M, Kumar P, Pillay V. Improved antioxidant, antimicrobial and anticancer activity of naringenin on conjugation with pectin. 3 Biotech. 2019;9(8):312.
30. Charmi J, Nosrati H, Amjad JM, Mohammadkhani R, Danafar H. Polyethylene glycol (PEG) decorated graphene oxide nanosheets for controlled release curcumin delivery. Heliyon. 2019;5(4):e01466.
31. Ma Y, Liu B. Preparation and α-glucosidase inhibitory activity of gallic acid-dextran conjugate. Natural Product Communications. 2020;15(8):1-5.